A Virtual Instrument for Time-Frequency Analysis of Park Power Components

Antonello Monti (+), Ferdinanda Ponci (+), Stefano Pelizzari (++), Loredana Cristaldi (++)

(+) Electrical Engineering Department, University of South Carolina, Columbia, SC (USA)
(++) Dipartimento di Elettrotecnica, Politecnico di Milano, Milano (Italy)

The paper is an extended version of paper presented at the Seventh International Workshop "Angelo Barbagelata" on Power Definitions and Measurements under Non-Sinusoidal Conditions, July 10-12, 2006, Cagliari, Italy.

Antonello Monti (contact author)
EE Department
University of South Carolina
301 S. Main St.
Columbia, SC (USA)
tel:+1-803-777-2722
fax: +1-803-777-8045
e-mail: monti@engr.sc.edu

Ferdinanda Ponci
EE Department
University of South Carolina
301 S. Main St.
Columbia, SC (USA)
tel:+1-803-777-7365
fax: +1-803-777-8045
e-mail: ponci@engr.sc.edu

Stefano Pelizzari
Dipartimento di Elettrotecnica
Politecnico di Milano
Piazza Leonardo da Vinci 32
20133 Milano (Italy)
tel:+39-02-2399-3715
fax: +39-02-2399-3703

Loredana Cristaldi
Dipartimento di Elettrotecnica
Politecnico di Milano
Piazza Leonardo da Vinci 32
20133 Milano (Italy)
tel:+39-02-2399-3715
fax: +39-02-2399-3703
e-mail: loredana.cristaldi@polimi.it

1. Summary

The paper presents an implementation of a virtual instrument to perform wavelet analysis on the Park Power components. A justification for the approach is presented, followed by the details about the specific implementation performed in the laboratory. Finally a preliminary testing activity based on the use of Hardware in the Loop approach is also presented.

2. Introduction

Load signature analysis has been widely studied in the last ten years. It is possible to define a progressive growth of complexity in the approach adopted.

One of the most significant changes has been the shift from quasi-steady-state analysis approaches to fully transient analysis.

A case for this shift is well made in [1]. While a steady-state analysis of the power components can be successfully completed in a residential environment, the same approach is very likely to fail in an industrial environment. The main reason for this failure is the fact that the signature-space becomes quickly crowded with undistinguishable loads.

The use of transient data widely enriches the amount of information available.

In a previous paper the authors presented an approach to the signature analysis based on the combination of the Park transform and a wavelet transformation [2].

The main ideas behind the approach are the following. In order to get significant signatures the usage of current or voltage is not enough. An interesting approach is proposed in [3], where the signature is reconstructed by using instantaneous power and current.

As already demonstrated in [2], through a set of examples a significant set of information can be reconstructed by the instantaneous components of the power in Park domain. A comprehensive analysis of the physical interpretation of these power components can be found in [4] and [5].

In [2], in order to cope with transient data, the Park power components have been analyzed through wavelet transformation.

The idea of using wavelet to analyze transient power has also been proposed in [6]and [7]. In this case though, the work focus on single phase systems and the usage of 90 degree shift filter is proposed to obtain information about reactive power.

However, wavelets are widely applied in power quality analysis [8] for the same reasons for which the authors believe can have a significant impact in the load signature analysis: possibility to analyze non-stationary components, multi-resolution capability.

In particular, by using dyadic-orthonormal bases we can extract significant information in the frequency domain analysis of power.

In section 9, different load conditions will be analyzed in order to extract the suitable set of information useful to define footprint characteristics.

In the following, we quickly report some simple remarks about Park Transformation and Wavelet and then we focus on the implementation of the algorithms in a distributed monitoring environment.

The details of the Labview implementations as well as data about the hardware adopted are reported.

Finally a hardware-in-the-loop (HIL) testing procedure is presented to validate the developed software.

The HIL experiment is based on the Virtual Test Bed (Real Time Extension) developed at the University of South Carolina. Thanks to this platform, as shown in the following, we have been able to replicate the scenarios adopted in [2] without the need of actually create a real flow of power but nevertheless using the real data acquisition system and the embedded hardware for measurement.

3. Park Domain and Wavelet Transform

The Park transformation can be applied, generally speaking, to any multi-phase system. In the simplest case we can focus on a three-phase scenario.

Given the three phase quantities x_a, x_b, and x_c the correspondent Park domain quantity is obtained applying a suitable matrix T to the vector X defined as:

$$X = \begin{bmatrix} x_a & x_b & x_c \end{bmatrix}^t$$

so that we obtain a new quantity in the new domain as:

$$X_p = TX$$

The vector X_p will have as well three elements that are defined as: direct, inverse and zero sequence.

If we focus on three wire systems we can disregard the zero sequence and introduce the so-called Park vector as:

$$\bar{x}_p = x_d + jx_q$$

The matrix T can be defined according to different criteria including the relative speed between the three-phase phasor and the reference Park system [7];In the following we adopt the following definition:

$$T = \frac{\sqrt{2}}{\sqrt{3}} \begin{bmatrix} \cos(0) & \cos\left(-\frac{2\pi}{3}\right) & \cos\left(-\frac{4\pi}{3}\right) \\ -\sin(0) & -\sin\left(-\frac{2\pi}{3}\right) & -\sin\left(-\frac{4\pi}{3}\right) \\ \frac{\sqrt{2}}{2} & \frac{\sqrt{2}}{2} & \frac{\sqrt{2}}{2} \end{bmatrix}$$

This matrix, that holds for the case of fixed Park reference, defines an orthonormal transformation so that:

$$T^{-1} = T^t$$

Given the definition of the transformation we introduce the power in the Park domain as the product between the voltage Park vector and the conjugate of the current Park vector:

$$\bar{p} = \bar{v}\bar{i}^* = (v_d + jv_q)(i_d - ji_q) =$$
$$= \left(v_d i_d + v_q i_q\right) + j\left(v_q i_d - v_d i_q\right)$$

Two comments complete this brief introduction:

- In the case of a steady-state sinusoidal system the real and imaginary part of the Park power are coincident with the classical active and reactive power
- Because of the properties of the transformation the power does not depend on the specific reference adopted (this is a classical propriety of any tensor analysis)

Following the approach proposed in [2] the instantaneous samples of *p(t)* and *q(t)* are then processed with wavelet transform to obtain time-frequency information.

Different wavelet bases can be adopted to perform the operation. In the previous paper we considered Haar wavelet and Malvar wavelet, while for the experimental implementation we focused on Haar and Daubechies transform.

The Haar wavelet basis is an orthogonal basis used in the applications described in the following sections. The Haar wavelet is defined as:

$$\psi(t)=\begin{cases}1 & 0\le t<1/2\\ -1 & 1/2\le t<1\\ 0 & otherwise\end{cases}$$

The other functions of the basis are obtained with rescaling and shifting of the so-called mother wavelet previously defined. In particular the other functions of the basis are obtained according to:

$$\psi_{j,k}(t)=2^{j/2}\psi\left(2^{j}t-k\right)$$

so that the scaling factor j turns the length of the support to 2^j, k is the shift factor and $2^{j/2}$ is the normalization factor.

The scaling function of the Haar wavelet system is defined as:

$$\varphi(t)=\begin{cases}1 & 0\le t<1\\ 0 & otherwise\end{cases}$$

This orthogonal system allows the decomposition of any $L_2(R)$ function into the sum of a coarse representation related to the scaling function, with an averaging meaning, and a sum of finer and finer details related to the wavelets [9].

4. Hardware structure of the measurements platform

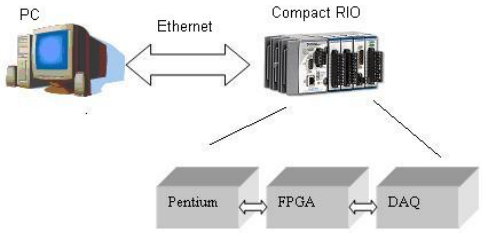

Figure 1: the HW structure used for the experiment

The hardware implementation is based on a standard desktop PC and a National Instrument Compact RIO (Figure 1).

The National Instruments Compact RIO 9002 is an embedded real-time controller that features an industrial 200-MHz Pentium-class processor for deterministic and reliable real-time applications. It contains 32 MB of DRAM memory and 64 MB of nonvolatile Compact Flash storage for file storage. It features a 10/100 Mb/s Ethernet port for programmatic communication over the network and built-in Web (HTTP) and file (FTP) servers. Using the remote-panel Web server, it is automatically possible to publish the front-panel graphical user interface of a LabView Real-Time application for multi-client remote monitoring or control. The Compact RIO-9002 also features dual 9 to 35 VDC supply inputs and low power consumption. The Compact RIO-9002 accepts 9 to 35 VDC power supply inputs on power-up and 6 to 35 VDC power supply inputs during operation. This device is an advanced embedded control and acquisition system powered by NI reconfigurable I/O (RIO) technology. The Compact RIO combines a low-power-consumption, real-time embedded processor with a high-performance RIO FPGA chipset. The device's core has built-in data transfer mechanisms to pass data to the embedded processor for real-time analysis, post processing, data logging, or communication to a networked host computer. The Compact RIO provides direct hardware access to the I/O circuitry of each I/O module using Lab View FPGA elementary I/O functions. Each I/O module includes built-in connectivity, signal conditioning, conversion circuitry (such as ADC or DAC), and an optional isolation barrier. This represents a low-cost architecture with open access to

low-level hardware resources. Each Compact Rio I/O module also contains screw terminals, BNC, or DSUB connectors. By integrating the connector junction box into the modules, the Compact RIO system significantly reduces the space requirements and field-wiring cost. Because the modules contain built-in signal conditioning for extended voltage ranges or for industrial signal types, the wiring connections can usually be made directly from the Compact RIO module to the sensors and actuators. This project uses only the analog input module (NI cRIO 9201).

5. Software Implementation: Labview Programming

The data are acquired using the analog input module 9201. Five channels are necessary (a total of eight is available). Three are used for the voltages and two are used for the currents, since the system has only three wires. The timing and processing of the acquisition is managed through the FPGA board inside the Compact RIO.

The overall software structure can be split in three main tasks:

- Task 1 is downloaded onto the FPGA. It performs the data acquisition. The processing at this level is based on integer numbers.
- Task 2 is downloaded onto the Compact Rio and is the main task. It performs the signal rescaling, voltage and current Park transform, calculation of the Park power components.
- Task 3 runs on the PC, and it performs the wavelet transform and the scalogram visualization.

5.1 FPGA Program

This task acquires the signal and stores the data in a buffer based on a FIFO structure where the time out is set on 0 (if the queue is full, the program waits until there is an empty space).

. Figure 2 shows the process of storage. .

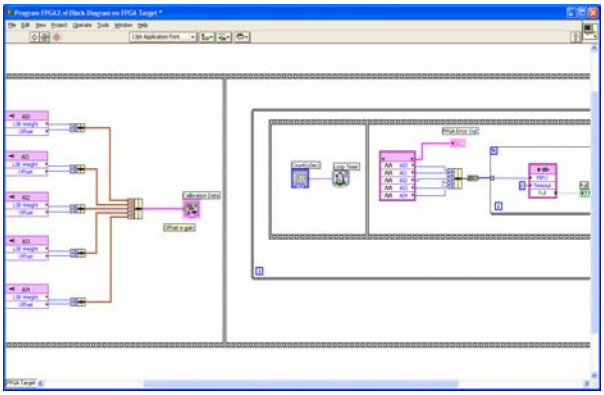

Figure 2: Block Diagram of the FPGA Program

5.2 Compact RIO Program

The Compact Rio program is the main component of the project. Because of limitations of the Real Time Operating System, the Compact RIO can not execute tasks with a sampling rate higher thank 1 kHz and then the algorithm can not be applied at a single sample. The problem is overcome by processing a batch of data stored in the FPGA FIFO (see Figure 3). In every cycle, 512 samples acquired with a sample frequency of 10kHz are elaborated for each channel. Consequently, every cycle lasts 51.2ms.

Inside the while loop, a block reads the FIFO where the data are stored. The number of elements read from the FIFO is 2560, or 512 samples for every channel. The size of the FIFO is higher than 2560. Thus, the samples are not lost. The “timeout” specifies the number of milliseconds that the VI waits before timing out. This case is set up on -1, meaning that the program waits until there are enough samples. Also, the “elements remaining” block returns the number of elements remaining in the host memory part of the FIFO.

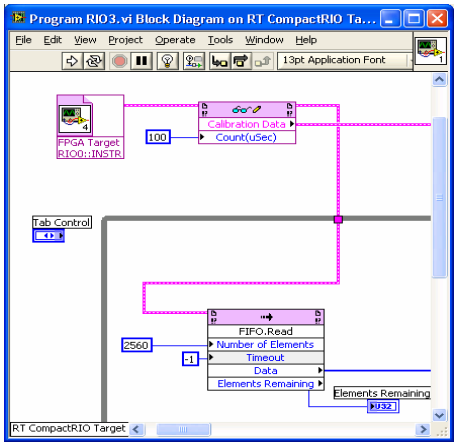

Figure 3: Reference to FPGA and FIFO on block diagram of the RIO program

The output data of the FIFO.read is an array of elements (2560) with the data from different channels. Then, the program executes three sequences in series shown in Figure 4. The first sequence involves taking the samples from the FIFO and redistributing them into the different channels. The second sequence converts binary to nominal. This operation must be done on the Compact RIO because the FPGA does not manage numbers in floating point format. This second sequence is made of six sub-sequences that rescale the signals (three for the voltage and three for the current). The sixth sub-sequence also computes the third current.

The last of these three consecutive sequences produces the fixed-axes Park transform The zero component is not calculated considering that we are working with a three–wire system. Finally, the last sequence simply computes the component of the power according to the Park reference

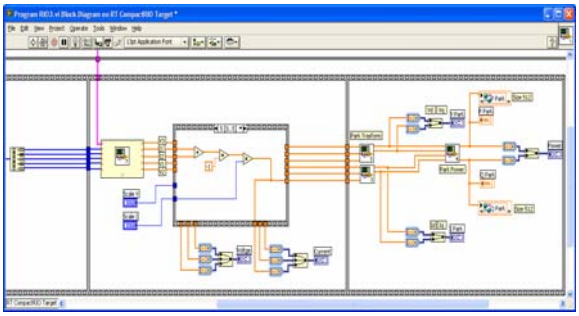

Figure 4: The sequences of the Compact RIO Program

The Compact RIO can also visualize both input and transformed signals.

The calculated values for the Park power components are stored in two buffers, one for the real power and the other for the immaginary power. The buffer stores the 512 points from every new cycle; thus, it is possible to obtain the current data after every cycle for an accurate real-time evaluation. At the end of this operation, the data are ready for the wavelet transform.

On the front panel the following data are available:

- Data: Buffers P and Q, scale parameters, and the elements remaining to fill the FIFO;
- Graphs: Input voltage, input current, the direct and squaring components of voltage, and these two components of current, and active and reactive Park power.

Figure 5 is an example of visualization of the three-phase voltages.

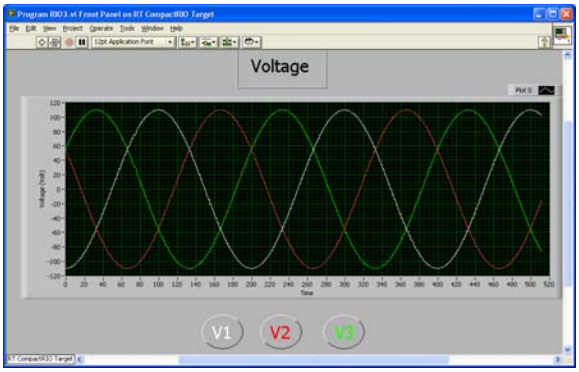

Figure 5: Three Phase voltages on the front panel of the Compact RIO program

5.3 Wavelet Program on PC

The data previously stored in the buffer may be read outside the Compact RIO, in a program on the PC. The last operation is the wavelet transform. The computational effort for this part may be significant and then it is better not to overload the RIO platform to be able to keep real-time constraints. The PC-based Labview program loads the buffer previously filled and computes the wavelet transform after every cycle of the Compact RIO program. The transformation is calculated by means of a set of Matlab-based routines executed in Labview thanks to the Labview/Matlab interface.

This solution allowed the authors to quickly port the software developed in the Matlab platform avoiding any possible coding error.

The output coefficients of the transform are sent to a 3D data visualization with color-map.

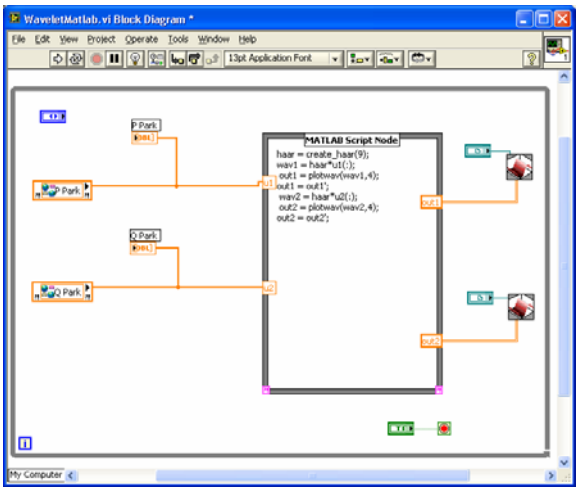

Figure 6: Block diagram of the wavelet program

6. Distributed Monitoring Feature

Thanks to the architecture described above the Virtual Instrument here proposed can be easily extended for a plant-distributed application.

Figure 7 shows the structure of the distributed measurement set-up. A set Compact-RIO can be used to collect data in specific plant locations. A single PC station can be used to perform the wavelet processing.

The RIO stations can also be dedicated to other local functions such as control of a local converter.

The data exchange is performed as in the case of the single station by means of FIFO buffer shared by the RIO over the network.

This solutions allows the seamless insertion of the monitoring feature in a more complex power distribution control system so that this kind of evaluation can be inserted within a more complex plant management structure [10].

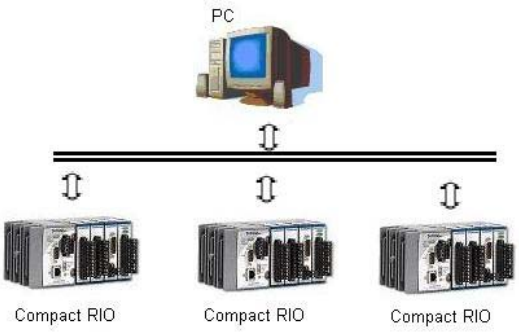

Figure 7: A RIO-based distributed monitoring structure

7. VTB Real Time and Hardware in the Loop Testing

Real-time HIL simulation replaces the emulated hardware under test or control logic in the simulation model with real hardware that interacts with the computer models. This increases the realism of the simulation and provides access to the hardware features currently not available in software-only simulation models, hence reduces the risks of discovering an error in the very last stage of the on-the-field testing [12][13]. Real-time HIL simulation has a wide application, such as power quality disturbances investigation, and modern automotive electronic control unit development.

Among the different platform even commercially available for HIL, VTB-RT has unique properties such as multi-platform, multi-solver, and hard real-time. Instead of competing with commercial systems, it is designed to provide a very low-cost alternative for real-time HIL applications while maintaining acceptable resolutions.

In VTB-RT, Linux and RTAI [16] were adopted as the underlying real-time operating system. On the other hand, VTB-RT is fully based on the VTB Technology developed at the University of South Carolina [14][15].

It reads the same file format created by the VTB schematic editor under Windows, thus makes it convenient to export simulations from the non-real-time platform, the VTB, into the real-time platform, the VTB-RT.

For what it concerns the work described in this paper, VTB-RT has been used to generate the testing data for the Virtual Instrument.

The schematics adopted for simulation in the previous paper have been executed in real time on the Linux platform to obtain real data out of Digital to Analog Converter board to be used as measurement for the new measurement platform.

The HW running VTB-RT is a PC desktop equipped with Pentium 4 at 2.8 GHZ, and with NI DAQ board NI PCI-6733.

The simulation scenarios have been executed with a time step of 100 microseconds to achieve enough details in the waveform reconstruction.

8. Experimental results

Here we report some examples of measurements performed by using the proposed architecture.

We focused the preliminary experimental activities on two cases one with distortion and one without.

The RT scenarios for the HIL simulation has been obtained porting to Linux some of the examples presented in [2].

Figure 8 shows the imaginary part of the Park power for a linear constant and equilibrated load. As expected, the q(t) has only component for the first level of decomposition and this quantity is constant.

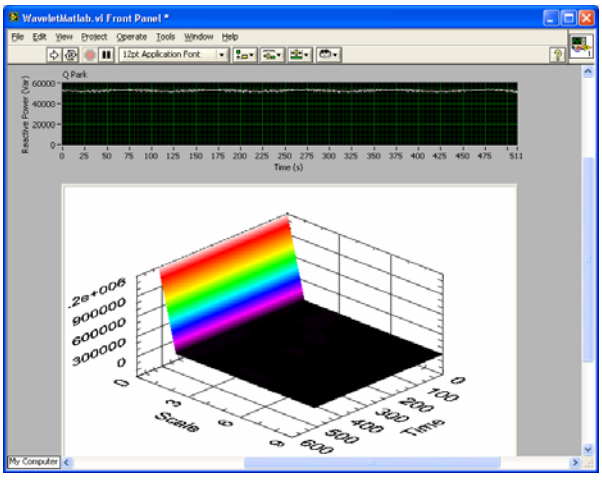

Figure 8: the wavelet 3D plot with 3-phase RL load

More interesting is the analysis of the example reported in Figure 9. In this case we have a three-phase distribution system connected to a reversible Graetz bridge.

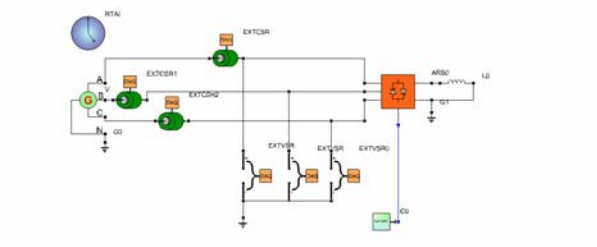

Figure 9: Schematic for the RT simulation of a reversible Graetz bridge.

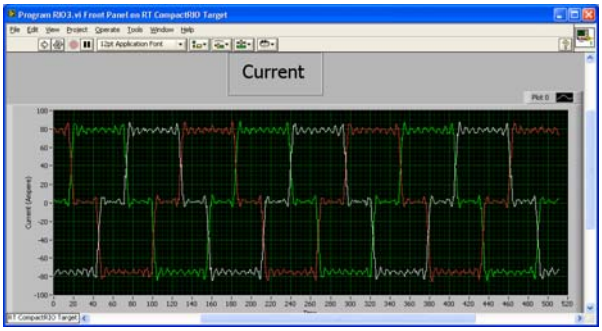

Figure 10: phase currents for the scenario in Figure 9

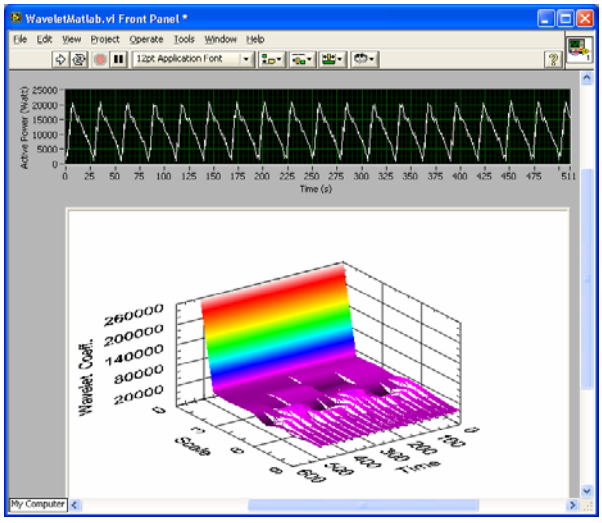

Figure 11: real part of the Park power for the schematic in Figure 9

During the execution of the RT scenario, the phase currents of Figure 10 have been acquired and coherently the Park power spectrum reported in Figure 11 has been evaluated for the real component. It is possible to verify that the time-frequency content matches the theoretical prediction made just using the standard simulation validating the HW implementation.

9. Load detection: experimental results

The next step is load detection: the process can be performed automatically recognizing the signatures described in the previous paragraph. The logic can be summarized through the following steps:

1) by analyzing the first level of Haar decomposition changes in the total real and imaginary power absorbed can be detected
2) if this change can be univocally related to a specific load, the process is completed
3) if more than one load could induce the same variation in the real and imaginary components, the signature must be analyzed.

In the following we focus only on this third stage which is the more challenging. Different cases (all using the Haar base) are presented:

- Detection of a linear balanced RL load
- Detection of a linear unbalanced RL load
- Detection of a three-phase Graetz bridge
- Detection of a linear RL load that changes from balanced to unbalanced (and other situations where the load changes);
- Detection of two loads: a linear balanced RL load and a linear unbalanced RL load (and other situations simultaneously involving more than one load)

9.1 Detection of a linear balanced RL load

In this case considering only the real power of a linear balanced RL load, a significant component appears on level zero of the wavelet decomposition. This component is constant in time. Load detection can be based on this feature.

The first column of the wavelet matrix is checked. A comparison is done between different sequences of 1024 values. If the variation is within a predefined range, a led indicating load detected is turned on. A range is used instead of a constant value because the amplitude is not exactly constant; rather, it varies slightly from one set of 1024 points to the next. To reduce the risk of errors in detection when other kinds of loads have the same zero component, other components must be checked to distinguish one kind of load from the other: in this case the signature requires that all the other components are approximately zero. Figure 12 gives the block diagram. When the load is turned on, a red light illuminates on the front panel, as shown in Figure 13.

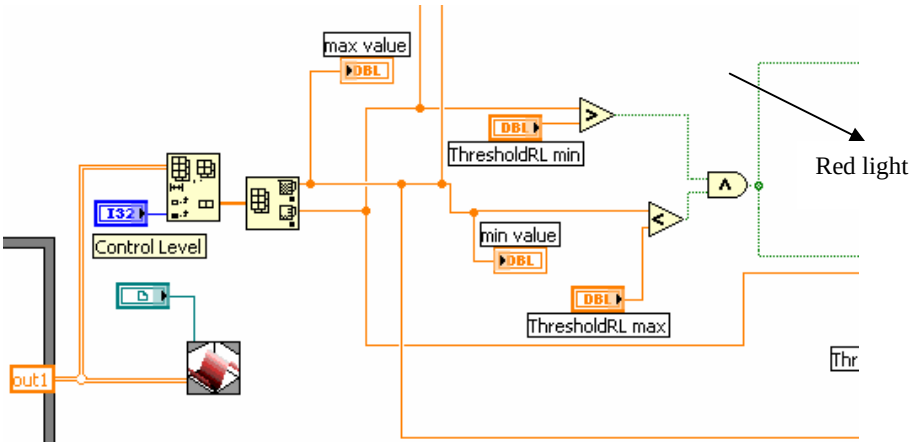

Figure 12: Block diagram with a balanced RL load detection.

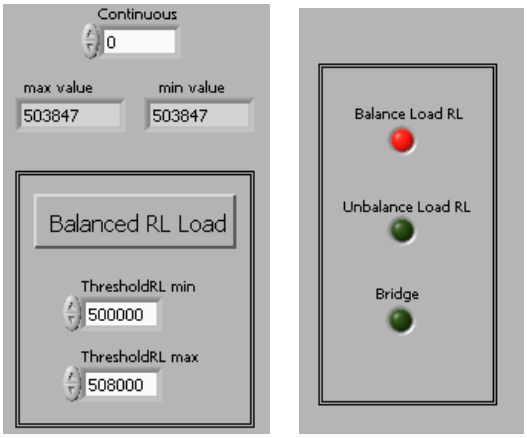

Figure 13: Front panel with a balanced RL load detection.

9.2 Detection of a linear unbalanced RL load

If a linear unbalanced load is connected, a significant component appears on the third level of decomposition, for both the real and imaginary power. This component is constant in time. The load detection is displayed in Figure 14. The third component is controlled in the case of imaginary power, and the third column is checked.

Implementing this load detection requires three conditions. First, the absolute value of the difference between the maximum and the minimum must be a small value, meaning that the component is constant (or close to constant). The second condition is that this component must be higher than a specified threshold so that the component is significant. The third condition is that level zero of the wavelet transform for the real power should not be the same as in any other combination of loads.

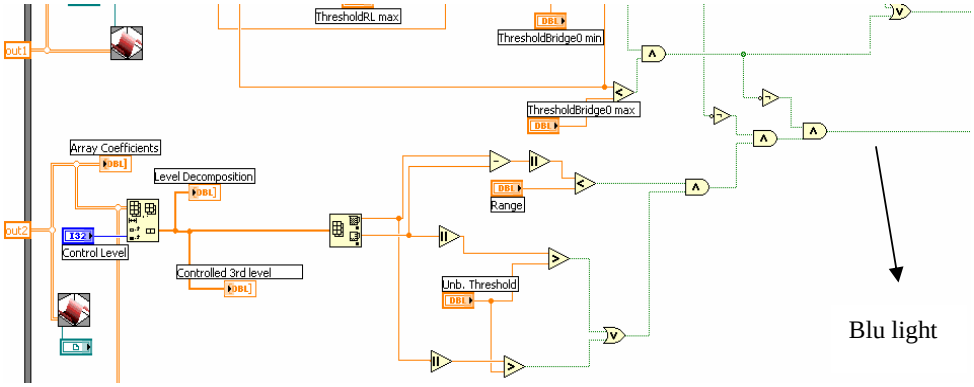

Figure 14: Block diagram with an unbalanced RL load detection.

9.3 Detection of a three-phase Graetz bridge

Detecting a three-phase Graetz bridge with an RL load is more difficult than detecting the previous two loads. For this bridge, the higher level of decomposition must also be controlled. The bridge is a nonlinear load and introduces high harmonics and distortion. The current is highly distorted with quasi-square wave behavior. The first, fifth and sixth levels of decomposition of the imaginary power's wavelet are checked in order to detect the load. After determining the features of the load, the following conditions can be established:

- The first level is constant; the maximum and minimum values must therefore be the same.
- The fifth and sixth levels are not constant but are significantly different from zero. The maximum and minimum values must be outside an interval.

The zero level of the real power's wavelet is also checked in the same way as for the previous two loads. The block diagram and the front panel are shown in Figure 15 and Figure 16.

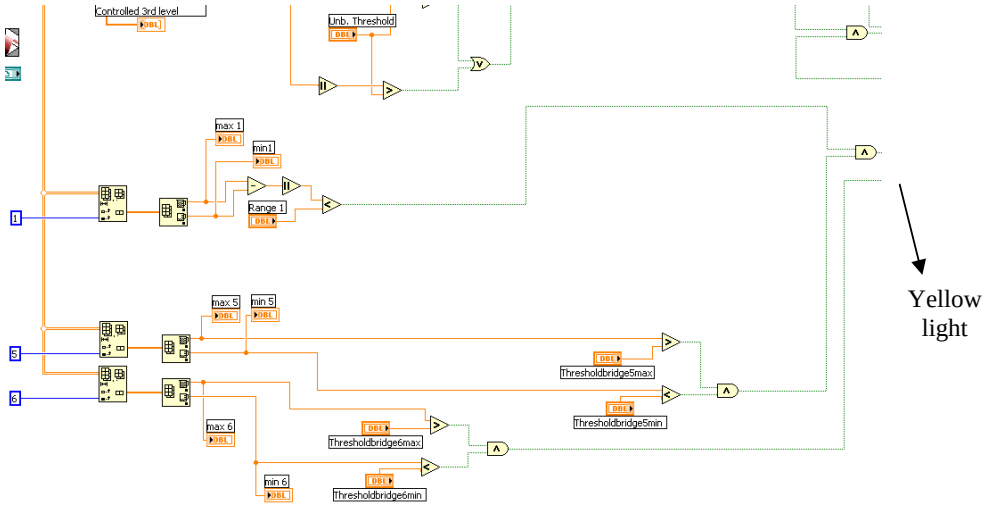

Figure 15: Block diagram with the bridge detection (I).

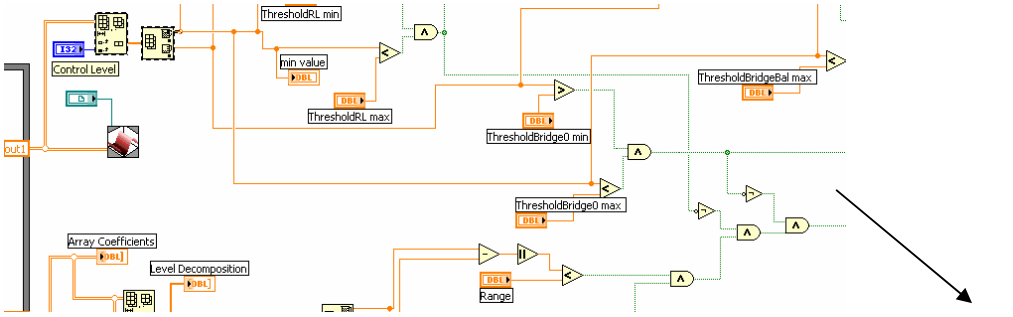

Figure 16 Block diagram with the bridge detection (II).

9.4 Detection of two loads: a linear balanced RL load and a linear unbalanced RL load

Another situation not yet discussed in this work is the simultaneous presence of two loads, e.g. a balanced load and an unbalanced load. In this case, level zero of the real power wavelet decomposition has a particular value indicating the presence of both loads. Therefore, the thresholds change. Using the same loads as in the previous simulations, the component on level zero is the sum of the separate components in the cases where the loads were alone. The unbalanced load is detected in the same way as before, with a control on the third level of decomposition. Figure 17 illustrates the block diagram and the front panel.

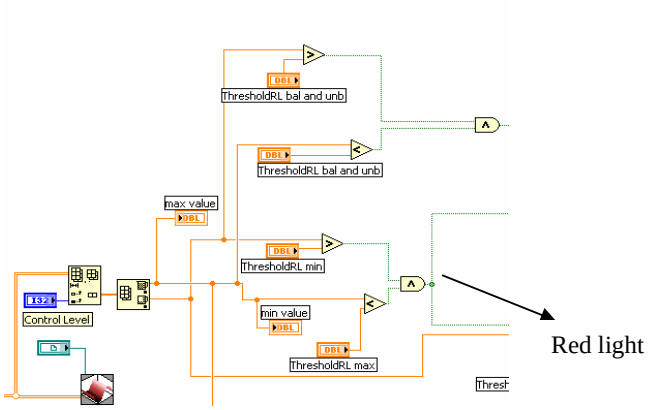

Figure 17: Block diagram showing the detection of balanced and unbalanced loads.

In the same way, the presence of two of the other loads can be detected: the balanced load and the bridge, and the unbalanced load and the bridge. In the first case, the presence of the balanced load and the bridge is detected because level zero has a particular value characteristic of the presence of both the loads. In addition, the bridge causes the presence of the higher components, which

therefore must be checked. In the second case, the unbalanced load is detected and the third level is controlled as before. The bridge is detected again because level zero assumes a particular value and because the case involves high frequency components.

10. Conclusions

This paper presented a virtual instrument for load detection to be used in a monitoring activity. The theory has been validated through an experimental activity performed with the support of a real-time simulation of the plant. Three different kinds of loads have been considered in performing load detection. Different combinations of these loads were shown and the load signature logics have been illustrated. This work demonstrated the possibility to realize load detection combining Park power component decomposition and wavelet analysis.

The situation could be more complicated inserting more loads with different characteristics.

In the future, the authors also plan to better exploit wavelet for the detection of load transient: this capability would extend the set of load that can be identified even under condition of equal absorption in steady state.

11. Acknowledgement

This work was supported by the U.S. Office of Naval Research under Grant N00014-02-1-0623.

REFERENCES

[1] Laughman, C.; Kwangduk Lee; Cox, R.; Shaw, S.; Leeb, S.; Norford, L.; Armstrong, P.; Power signature analysis, Power and Energy Magazine, IEEE , Volume: 1 Issue: 2 , March-April 2003 Page(s): 56 -63A.

[2] Cristaldi L., Monti A., Ponci F., "Three-phase Load Signature: a wavelet-based approach to power analysis", Sixth International Workshop on Power Definitions and Measurements under Non-Sinusoidal Conditions, Milano, October 13-15, 2003

[3] Legowski, S. F., Sadrul Ula A. H. M., and Trzynadlowsh A. M., "Istantaneous Power as a Medium for the Signature Analysis of Induction Motors", on IEEE Trans. on Industry Applications, vol. 32, No. 4, July/August 1996, pp. 904-909

[4] A. Ferrero, G. Superti Furga, "A New Approach to the Definition of Power Components in Three-Phase System Under Nonsinusoidal conditions", on IEEE Trans. on Instrumentation and Measurements, vol. 40, N. 3, June 1991, pp. 568-578

[5] L. Cristaldi, A. Ferrero, G. Superti-Furga, "Current Decomposition in Asymmetrical, Unbalanced Three-Phase Systems Under Nonsinousoidal Conditions", on IEEE Trans. on Instrumentation and Measurements, vol. 43, N. 1, February 1994, pp. 63-68

[6] W. Yoon and M. J. Devaney, "Reactive Power Measurement Using the Wavelet Transform", on IEEE Trans. on Instrumentation and Measurements, vol. 49, N. 2, April 2000, pp. 246-252.

[7] W. Yoon and M. J. Devaney, Member, "Power Measurement Using the Wavelet Transform", IEEE Transactions On Instrumentation And Measurement, Vol. 47, N. 5, October 1998, pp. 1205-1210

[8] S. Santoso, E. J. Powers, W. M. Grady, P. Hofmann, "Power Quality Assessment via Wavelet Transform Analysis", IEEE Transaction on Power Delivery, vol. 11, n. 2, April 1996, pp. 924-930

[9] Vetterli M., Kovacevic J., "*Wavelets and subband coding*", Prentice Hall, 1995

[10] L. Cristaldi, A. Monti, F. Ponci, "Power Quality Indeces in an Agent-based Reconfiguration Strategy for Ship Power Systems", in Proc. of VI International Workshop on Power Definition and Measurements under non-sinusoidal conditions, June 10-12 2006, Cagliari (Italy)

[11] B Lu, X. Wu, H Figueroa, “A Low Cost Real-Time Hardware-In-the-Loop Testing Approach of Power Electronics Controls”, on printing for IEEE Trans. on Industrial Electronics
[12] B. Lu, A. Monti, and R. Dougal, “Real-time hardware-in-the-loop testing during design of power electronics controls,” in Proc. 29th Annual Conference of the IEEE Industrial Electronics Society (IECON’03), vol. 2, Nov. 2003, pp.1840-1845
[13] X. Wu, H. Figueroa, and A. Monti, “Testing of digital controllers using real-time hardware in the loop simulation,” in Proc. 35th IEEE Power Electronics Specialists Conference (PESC’04), vol. 5, June 2004, pp.3622-3627.
[14] Monti A., Santi E., Dougal R., Riva M., Rapid Prototyping of Digital Controls for Power Electronics, *IEEE Trans. On Power Electronics*, May 2003
[15] Dougal R., Lovett T., Monti A., Santi E., A Multilanguage Environment For Interactive Simulation And Development Of Controls For Power Electronics, *IEEE PESC01*, Vancouver (Canada).
[16] RTAI website, http://www.rtai.org/